Multiphonon resonant Raman scattering of light in quasi-two-dimensional electron systems

L. I. Korovin, S. T. Pavlov, and B. É. Éshpulatov

A. F. Ioffe Physicotechnical Institute, Academy of Sciences of the USSR, Leningrad
(Submitted 6 November 1990)
Zh. Eksp. Teor. Fiz. **99**, 1619–1631 (May 1991)

A manyfold increase in the intensity (by a factor of α^{-1}, where α is the dimensionless electron–phonon interaction constant obeying $\alpha \ll 1$) is predicted for multiphonon resonant Raman scattering of light in quasi-two-dimensional electron systems (quantum wells, inversion layers), compared with a bulk semiconductor. The amplification threshold is shifted from four-phonon scattering (in the bulk) to three-phonon scattering in the two-dimensional case.

1. INTRODUCTION

Perfect quasi-two-dimensional electron structures (inversion layers, heterostructures, quantum wells) can now be formed in semiconductors. This has stimulated major interest in physical properties of quasi-two-dimensional electrons. An important place in the current investigations of the topic is held by the method of resonant Raman light scattering (RRLS) involving optical (LO) phonons.[1] Such scattering was first observed in a GaAs/AlGaAs superlattice at room temperature.[2,3] In the case of a bulk semiconductor subjected to illumination with light from the fundamental absorption region it is found that the secondary radiation (luminescence) spectrum has a series of lines known as the phonon replicas and located at frequencies satisfying the condition

$$\omega_s = \omega_l - N\omega_{LO}, \tag{1.1}$$

where ω_l is the frequency of the laser (exciting) light; ω_{LO} is the LO phonon frequency; N is the number of phonons emitted in a scattering event or the phonon replica number. This is known as multiphonon resonant Raman light scattering (MRRLS). The intensity of the phonon replica peaks falls slowly on increase in N, so that experiments can reveal distant phonon replicas. For example, in the case of InI the phonon replicas had been observed right up to $N = 20$ (Ref. 4).

The weak dependence of the phonon replica peak intensity on its number can be explained qualitatively as follows.[5] We shall assume that the absorption of light of frequency ω_l creates an electron–hole pair (EHP). The energy of the electron in such a pair is released generating LO phonons and it finally annihilates with a hole, emitting the last phonon of the cascade and scattered light of frequency ω_s [see Eq. (1.1)]. A different scattering channel is also possible and in this case the creation of an EHP is accompanied by phonon emission (indirect creation); then, in real transitions phonons are emitted and, finally, an EHP annihilates directly. We shall consider phonon replicas with numbers $N \geqslant 4$. The emission of phonons results in a real random walk of an electron in the bulk and the mean free path is $l \propto \alpha_0^{-1}$, where α_0 is the Fröhlich electron–phonon coupling constant. In the case of direct annihilation (i.e., for equal momenta of an electron and a hole) the cross section σ_N of the MRRLS process is proportional to the probability of return of an electron to the point of creation of an EHP after the emission of $N-1$ phonons (for simplicity, we shall assume that the hole is heavy and that it remains at the point of creation of the EHP). The probability of this process is inversely proportional to the volume within which an electron random walk takes place. The most probable random-walk volume is $V_{\text{EHP}} \approx l^3 \propto \alpha_0^{-3}$, so that the cross section for the appearance of Nth phonon replica is $\sigma_{N>4} \propto \alpha_0^3$ and the tube of α_0 is independent of N (Refs. 6 and 7). In the case of lower values of N, where the above analysis does not apply, we have $\sigma_2 \propto \alpha_0^2$ (Ref. 5) and $\sigma_3 \propto \alpha_0^3 \ln \alpha_0^{-1}$ (Ref. 8).

Restrictions on the free motion of an electron lead, as is well known, to enhancement of the resonant effects. In a strong magnetic field, when the free motion of an electron is limited to one dimension, the MRRLS cross section rises strongly and we have $\sigma_{N>2} \sim \alpha_0$ (Ref. 9). This enhancement of the MRRLS in a magnetic field had been confirmed experimentally.[10] A magnetic field suppresses the electron–phonon interaction in a plane perpendicular to **H**; this increases the rate of exciton creation and, consequently, increases the intensities of the exciton luminescence lines, as described in Ref. 11. An electron in a quantum well can move freely only in the plane of the well. We can expect the reduction in the dimensionality of the system to result in a strong manyfold increase in the MRRLS cross section, compared with the case of similar scattering in a bulk semiconductor. In this case an electron emits phonons and wanders at random in the plane of a well over an area of the order of $l^2 \propto \alpha_0^2$, i.e., instead of the dependence $\sigma_N \propto \alpha_0^3$, we can expect

$$\sigma_N \propto \alpha_0^2. \tag{1.2}$$

It therefore follows that in a quantum well the MRRLS cross section should increase by the factor α_0^{-1} (Ref. 12). The specific behavior of phonon replicas in a quasi-two-dimensional quantum system is tackled in the present paper by developing a theory of the MRRLS by quasi-two-dimensional electron systems in the specific case of a quantum well. Our calculations are based on a general expression for the differential cross section representing the scattering by a quasi-two-dimensional system, such as a quantum well or an inversion layer in an MIS structure.[13] The intermediate states in the scattering process are EHPs. The exciton states, which can also act as intermediate states, make a much smaller contribution (see Ref. 14 and the literature cited there).

 0038-5646/91/050904-08$03.00

2. MODEL OF A QUANTUM WELL AND PRINCIPAL RELATIONSHIPS

Our theory will be developed for a quantum well with infinitely high potential barriers subject to the condition

$$d \ll l, \tag{2.1}$$

where d is the width of the quantum well. The motion of electrons and holes then becomes quantized at right-angles to the wall plane. It is assumed that the wall is bounded by the planes $z = 0$ and $z = d$. The energies of an electron (e) and a hole (h) are described by the following expressions:

$$\begin{aligned} \hbar\omega_{\mathbf{k}_e}{}^{e} &= \hbar\omega_{n_e}{}^{e} = \pi^2\hbar^2 n_e{}^2/2m_e d^2 + \hbar^2 k_e{}^2/2m_e, \\ \hbar\omega_{\mathbf{k}_h}{}^{h} &= \hbar\omega_{n_h}{}^{h} = \hbar\omega_g + \pi^2\hbar^2 n_h{}^2/2m_h d^2 + \hbar^2 k_h{}^2/2m_h, \end{aligned} \tag{2.2}$$

where $m_{e(h)}$ is the effective mass of an electron (hole); $\mathbf{k}_{e(h)}$ is the two-dimensional vector $\mathbf{k} = (k_x, k_y, 0)$; $n_{e(h)}$ are the quantum numbers of size quantization. The wave functions $\psi_{e(h)}$ of an electron and a hole are

$$\psi_{e(h)} = (2/S_0 d)^{1/2} \exp(i\mathbf{k}_{e(h)}\mathbf{r}) \sin(\pi n_{e(h)} z/d), \tag{2.3}$$

where $\mathbf{r}$ is a two-dimensional vector in the well plane; S_0 is the normalization area.

The general expression for the differential cross section for the scattering by a quasi-two-dimensional electron system[13] is

$$\frac{d^2\sigma}{d\omega\, d\Omega} = \sum_{\beta,\beta',\gamma,\gamma'} G_{\beta'\beta}(\omega_s) S_{\beta\gamma\beta'\gamma'}(\omega_l, \omega_s) J_{\gamma'\gamma}(\omega_l). \tag{2.4}$$

Second-rank tensors $G_{\beta'\beta}$ and $J_{\gamma'\gamma}$ are governed by the geometries of the scattered and incident waves, respectively; Ω is a solid angle. The fourth-rank scattering vector $S_{\beta\gamma\beta'\gamma'} \equiv S$ depends on the properties of the scattering region and is related to a product of the current commutators[15]

$$\begin{aligned} S = \frac{\omega_s}{\omega_l} c^{-4}\hbar^{-2} &\int_{-\infty}^{\infty} \frac{dt}{2\pi} \exp[i(\omega_l - \omega_s)t] \\ &\times \int_{-\infty}^{\infty} d\tau\theta(-\tau)\exp(-S_l\tau) \int_{-\infty}^{\infty} d\tau'\theta(-\tau') \\ &\times \exp(-S_l{}^*\tau') \langle [j_{\gamma'}{}^*(t+\tau'),\ j_{\beta'}{}^*(t)]\,[j_\beta(0), j_\gamma(\tau)] \rangle, \\ S_l = i\omega_l - \delta, \quad \delta &\to 0; \end{aligned} \tag{2.5}$$

where

$$\theta(x) = \begin{cases} 1, & x \geqslant 0, \\ 0, & x < 0, \end{cases}$$

and

$$j_\alpha(t) = \sum_{n,n'} j_\alpha^{nn'} (a_n{}^+ c_{n'}{}^+ + a_n c_{n'})_t \tag{2.6}$$

is a component of the current density operator; c is the velocity of light in vacuum; $(\ldots)_t$ denotes the Heisenberg representation; the operators a_n^+, and a_n' represent electrons in the conduction band; $c_n'^+$ and c_n represent holes in the valence band. In Eq. (2.5) the angular brackets $\langle \ldots \rangle$ denote averaging over the ground state of the electron system (at zero absolute temperature). The theory is linear in respect of the exciting light intensity.

In the MRRLS the optical transitions are of the interband type, since the frequencies ω_l and ω_s lie in the fundamental absorption region. Therefore, in the effective mass approximation using the dipole approximation, we find that

$$j_\alpha^{nn'} = \frac{e}{m_0} p_\alpha \delta_{n,n'}, \qquad \delta_{n,n'} = \delta_{n_e,n_h}\delta_{\mathbf{k}_e,-\mathbf{k}_h}, \tag{2.7}$$

where m_0 is the mass of a free electron; p_α is the projection of the interband matrix element of the momentum calculated using the Bloch modulating factors.

In a heterostructure there are not only bulk phonons, but also surface phonons (vibrations of the boundaries separating the layers) and slab phonons, which propagate in a given layer and are quantized for the motion across the layer. The interaction of electrons with different types of phonons is reflected in the characteristics of the MRRLS spectra, particularly the values of the secondary radiation frequencies ω_s. Moreover, some role may be played also by the mutual influence of bulk and quantized phonons. Combinations of different types of phonons also participate in the MRRLS processes. An analysis of the characteristics of the phonon spectrum and of the electron–phonon interaction listed above is outside the scope of the present treatment: we shall confine ourselves to an allowance for the interaction of electrons with just the bulk *LO* phonons. We shall use the experimental data demonstrating the dominant role of the bulk *LO* phonons in the RRLS processes that occur in superlattices made of heterostructures.[16]

The Hamiltonian of the electron–phonon interaction is

$$\mathcal{H}_{\text{int}}^{e} = \sum_{i,i'} \sum_{\mathbf{Q}} \{C_Q{}^e J_{ii'}(\mathbf{Q})\, b_Q a_i{}^+ a_{i'} + \text{H.c.}\}, \tag{2.8}$$

where b_Q and b_Q^+ are the phonon operators. The following notation is used in Eq. (2.8):

$$C_Q{}^e = -i\hbar\omega_{LO}(4\pi\alpha_0 l_0{}^3/V_0)^{1/2}(l_0 Q)^{-1}, \quad l_0 = (\hbar/2m_e\omega_{LO})^{1/2}, \tag{2.9}$$

$\mathbf{Q} = (\mathbf{q}, q_z)$; $\mathbf{q}$ and ω_{LO} are the two-dimensional wave vector and the frequency of a phonon; V_0 is the normalization volume. The operator representing the interaction of holes with phonons is derived from Eq. (2.8) by the substitution $a_i{}^+ a_{i'} \to c_i{}^+ c_{i'}$ and we have

$$C_Q{}^e \to C_Q{}^h = (C_Q{}^e)^* = -C_Q{}^e. \tag{2.10}$$

The functions $J_{ii'} - (\mathbf{Q}) \equiv J_{n_i k_i, n_{i'} k_{i'}}$ are given by the expressions

$$J_{n_i\mathbf{k}_i,\, n_{i'}\mathbf{k}_{i'}}(\mathbf{Q}) = M_{n_i n_{i'}}(q_z)\,\delta_{\mathbf{k}_i,\, \mathbf{k}_{i'}+\mathbf{q}}, \tag{2.11}$$

$$M_{n_i n_{i'}}(q_z) = \frac{2}{d}\int_0^d dz \exp(iq_z z) \sin\left(\frac{\pi n_i z}{d}\right) \sin\left(\frac{\pi n_{i'} z}{d}\right). \tag{2.12}$$

In addition to the Fröhlich interaction of Eq. (2.8), we shall consider a model interaction, in which C_Q is independent of the wave vector Q (Ref. 6), i.e.,

$$C_Q{}^e \equiv C^e = -i\hbar\omega_{LO}(4\pi A d^3/V_0)^{1/2}, \quad C^h = -C^e. \tag{2.13}$$

The tensor S can be represented by a sum of the contributions made by different phonon replicas:

$$S=\sum_N S^{(N)}. \tag{2.14}$$

The resonance frequencies at which phonon replicas with different values of N are observed are not all identical, as is clear from Eq. (1.1). In the calculation of $S^{(N)}$ it is convenient to use a diagram technique developed in Refs. 17 and 18 for the MRRLS in a bulk semiconductor. In the case of a quasi-two-dimensional system considered here the rules for constructing such diagrams are as follows.

1. An ordering contour C (dash-dot line in all the figures) consists of two regions located to the left (C_1) and right (C_2) of a section f (final state).

2. The electron lines pass above the contour C and the hole lines below it. These lines are continuous in our figures.

3. The wavy lines represent phonons and the dashed lines represent the exciting and scattered light. These lines do not correspond to any specific objects.

4. The lines joining the vertices inside the regions C_1 and C_2 are called inner and the lines connecting the vertices in different parts are called outer.

5. In the MRRLS all the electron and hole lines are inner. The inner electron (hole) lines in the region C_1 correspond to an electron (hole) retarded Green function $iG_e(n,\omega)$ [$iG_h(n,\omega)$], whereas in the region C_2 they correspond to the electron (hole) advanced Green function $iG(n,\omega)$ [$-iG_h(n,\omega)$].

6. The open circles denote the vertices of the electron–phonon interaction. In the region C_1 each vertex γ corresponds to a factor $(e/m_0)p_\gamma\delta_{\mu\mu'}$, where μ and μ' are the quantum numbers of the electron and hole lines entering or leaving a vertex. In the region C_2 the vertices correspond to complex-conjugate quantities.

7. The filled circles represent the vertices of the electron–LO-phonon interaction. If in the region C_1 an electron line μ enters a vertex, whereas an electron line ν and a phonon line $\mathbf{Q}$ leave the vertex, this vertex corresponds to a factor $(-i/\hbar)(C_Q^e)^*J_{\nu\mu}(-\mathbf{Q})$, whereas in the region C_2 it corresponds to a factor $(i/\hbar)C_Q^eJ_{nm}(\mathbf{Q})$, where m and n apply to the electron lines entering and leaving a vertex, respectively. In the case of the hole lines the quantity C_Q^e is replaced with $C_Q^h=-C_Q^e$.

8. The summation is carried out over the quantum numbers of the electron and hole lines, and also over the phonon wave vectors.

9. The integration is carried out with respect to the frequencies ω, ω' from $-\infty$ to ∞ with the weight $(2\pi)^{-1}$.

10. The section f corresponds to a factor $\delta(\omega_l-\omega_s-N\omega_{LO})$, where N is the number of the phonon lines that cross the section f, i.e., the number of phonon replicas.

11. Each graph is multiplied by $(\omega_s/\omega_l)c^{-4}\hbar^{-2}$.

These rules for the calculation of the contributions made to the tensor S by different phonon replicas are valid at $T=0$, when the conduction band is empty, the valence band is filled, the optical phonons are not excited, and the electron–phonon interaction involves spontaneous phonon emission. The dispersion of the LO phonons is ignored and the momentum of a photon participating in an interband transition is neglected. The electron and hole Green functions are

$$G_e(n,\omega)=(\omega-\omega_n{}^e+i\gamma_n{}^e)^{-1},\ G_h(n,\omega)=(\omega-\omega_n{}^h+i\gamma_n{}^h)^{-1},$$
$$\bar{G}_e(n,\omega)=G_e^*(n,\omega),\ \bar{G}_h(n,\omega)=G_h^*(n,\omega). \tag{2.15}$$

The Green functions contain the quantities γ_n^e and γ_n^h which represent the reciprocals of the lifetimes of the electron and hole states in the case of different scattering mechanisms. In particular, such a mechanism can be the interaction with the LO phonons. We shall not calculate γ_n^e and γ_n^h, but assume them to be constant, independent of the continuous quantum numbers, and satisfying the inequalities

$$\gamma_n{}^e,\ \gamma_n{}^h\ll\omega_{LO}. \tag{2.16}$$

In our estimates we shall use the obvious condition $\gamma_n^e\propto\alpha_0$ and $\gamma_n^h\propto\alpha_0$ (because of the proportionality to A in the model interaction). All the reported calculations were carried out in the approximation of a heavy hole, when the following inequalities apply:

$$\omega_n{}^h\ll\omega_{LO},\ \gamma_n{}^h\ll\gamma_n{}^e,\ (\omega_n{}^h-\omega_g)\ll\omega_n{}^e. \tag{2.17}$$

3. SECOND PHONON REPLICA

We shall consider graphs with two outer phonon lines which apply to the second phonon replica ($N=2$) in MRRLS (in the dipole approximation the first phonon replica is missing). We shall avoid cumbersome figures by including not the whole graph, but only its elements corresponding to the regions C_1 and C_2. Obviously, in the case of the second phonon replica there are three-elements which when connected give all the graphs. We shall denote these elements by a, b, c (Fig. 1). There is a total of nine connections (aa, ab, ac, ba, bb, bc, ca, cb, and cc) which correspond to nine types of graphs. Two outer phonon lines in each graph either do not intersect (diagrams a_1a_1, a_1b_1, etc.) or they do intersect (graphs a_2a_2, etc.), as demonstrated in Fig. 2.

We shall first show that the graphs of one type (a_1a_1 and a_2a_2, etc.) are equal. Summing with the aid of the δ symbols and integrating with respect to ω and ω', we obtain the contribution of the graph a_1a_1 (Fig. 2a) to the tensor $S^{(2)}$:

$$S^{(2)}_{a_1a_1}=B\delta(\omega_l-\omega_s-2\omega_{LO})$$
$$\times\sum_{n_\mu n_\nu n_n n_m}\sum_{\mathbf{k}_\mu\mathbf{k}_\nu}\sum_{q} I^{n_n n_m}_{n_\mu n_\nu}(q)\,I^{n_m n_n}_{n_\mu n_\nu}(q)$$
$$\times G_e(n_\mu,\ \mathbf{k}_\mu,\ \omega_0)\,G_e(n_\nu,\ \mathbf{k}_\mu-\mathbf{q},\omega_1)\,G_e$$
$$\times(n_\mu,\ \mathbf{k}_\mu,\ \omega_2)\,\bar{G}_e(n_n,\ \mathbf{k}_n,\omega_0)\,\bar{G}_e(n_m,\ \mathbf{k}_n$$
$$+\mathbf{q},\omega_1)\,\bar{G}_e(n_n,\mathbf{k}_\nu,\omega_2), \tag{3.1}$$
$$\omega_{N_0}=\omega_l-\omega_g-N_0\omega_{LO},\ N_0=0,\ 1,\ 2, \tag{3.2}$$
$$B=(\omega_s/\omega_l)(e/m_0c)^4\hbar^2p_\gamma p_\beta p_{\gamma'}{}^*p_{\gamma'}{}^*. \tag{3.3}$$

The function $I^{n_n n_m}_{n_\nu n_\mu}(q)$ is defined as follows:

$$I^{n_n n_m}_{n_\nu n_\mu}(q)\equiv I(q)=\hbar^{-2}\sum_{q_z}|C_Q|^2M_{n_\nu n_\mu}(-q_z)\,M_{n_n n_m}(q_z). \tag{3.4}$$

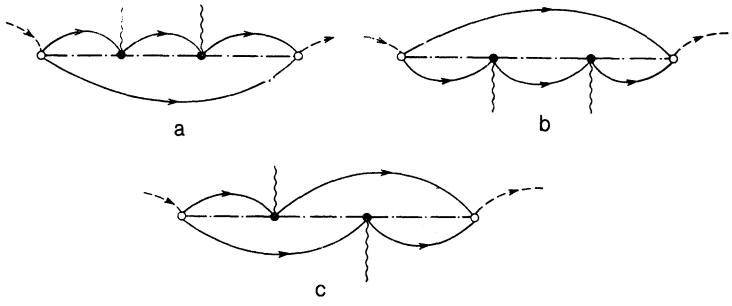

FIG. 1. Elements of graphs corresponding to the second phonon replica.

The graph a_2a_2 (Fig. 2b) differs from a_1a_1 by one function $I(q)$: instead of $I^{n_m n_n}_{n_\mu n_\nu}$, we now have $I^{n_n n_m}_{n_\mu n_\nu}(q)$. It follows from the definitions given by Eqs. (3.4) and (2.12) that the function $I(q)$ is symmetric under index transposition:

$$I_{ij}^{kl}(q)=I_{ji}^{kl}(q)=I_{ij}^{lk}(q)=I_{kl}^{ij}(q), \tag{3.5}$$

which yields also the equality $S^{(2)}_{a_1a_1}=S^{(2)}_{a_2a_2}$. Similar equalities apply also to the other graphs. In the graphs *ac*, *bc*, *ca*, and *cb* the number of the constants C^h_Q is odd, in contrast to the graphs *aa*, *bb*, *ab*, *ba*, and *cc*, in which case the number is even. Therefore, these two groups of graphs differ in respect of the sign. Allowing for this circumstance, we can easily prove that

$$\begin{aligned} &S^{(2)}_{ee}=4S^{(2)}_{aa}, \quad S^{(2)}_{ea}=S^{(2)}_{ae}=-2S^{(2)}_{aa}, \\ &S^{(2)}_{ea}=-2S^{(2)}_{a\bar{a}}, \quad S^{(2)}_{\bar{a}e}=-2S^{(2)}_{\bar{a}a}, \end{aligned} \tag{3.6}$$

which leads to the condition of mutual canceling of graphs:

$$S^{(2)}_{ae}+S^{(2)}_{ea}+S^{(2)}_{aa}=0.$$

Therefore, all the second-order graphs reduce to the following sum:

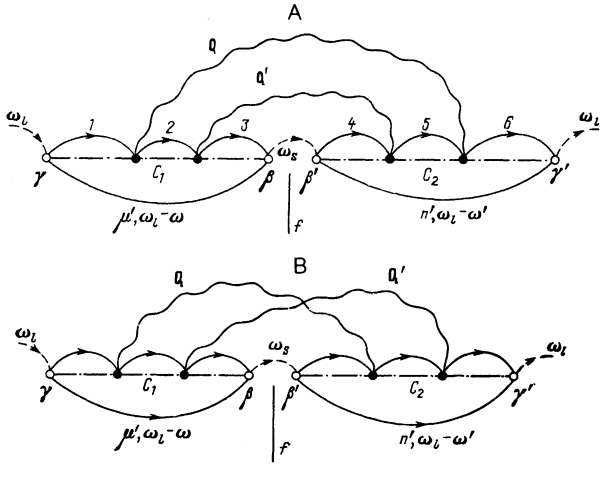

FIG. 2. Example of a comparison of graphs for the second phonon replica carried out using the element *a*: *A* is the a_1a_1 graph and *B* is the a_2a_2 graph. The indices of the electron states in the graphs a_1a_1 and a_2a_2 are identical. The Green functions 1–6 in the graph a_1a_1 correspond to the following quantities: 1) μ, ω; 2) ν_0, $\omega-\omega_{LO}$; 3) ν', $\omega-2\omega_{LO}$; 4) n', $\omega'-2\omega_{LO}$; 5) m, $\omega'-2\omega_{LO}$; 6) n, ω'.

$$S^{(2)}=2(S^{(2)}_{aa}-S^{(2)}_{a\bar{a}}-S^{(2)}_{\bar{a}a}+S^{(2)}_{\bar{a}\bar{a}}). \tag{3.7}$$

In the approximation of a heavy hole all these graphs contain monotypic products of the electron wave functions

$$\begin{aligned} A_1(n_\mu, n_\nu, q)&\equiv A_1 \\ &=\sum_{\mathbf{k}_\mu} G_e(n_\mu, \mathbf{k}_\mu, \omega_0)\, G_e(n_\nu, \mathbf{k}_\mu-\mathbf{q}, \omega_1)\, G_e(n_\mu, \mathbf{k}_\mu, \omega_2), \\ A_2(n_\mu)&\equiv A_2=\sum_{\mathbf{k}_\mu} G_e(n_\mu, \mathbf{k}_\mu, \omega_0)\, G_e(n_\mu, \mathbf{k}_\mu, \omega_1)\, G_e(n_\mu, \mathbf{k}_\mu, \omega_2), \\ A_1(n_\mu, n_\mu, 0)&=A_2(n_\mu). \end{aligned} \tag{3.8}$$

In terms of the new notation, $S^{(2)}$ can be reduced to

$$\begin{aligned} S^{(2)}=2B\delta(\omega_l-\omega_s-2\omega_{LO}) &\times \sum_{n_\mu n_\nu n_n n_m} \sum_q [I^{n_m n_n}_{n_\mu n_\nu}(q)]^2 [A_1(n_\mu, n_\nu, q)-A_2(n_\mu)] \\ &\times [A_1(n_n, n_m, q)-A_2(n_n)]^*. \end{aligned} \tag{3.9}$$

According to the definition given by Eq. (3.9), the function $I(q)$ for the Fröhlich electron–phonon interaction assumes the following form after integration with respect to the transverse phonon momentum q_z:

$$\begin{aligned} I^{mm'}_{nn'}(q)=\frac{8\pi\alpha_0 l_0 \omega_{LO}^2}{S_0 q d^2} &\int_0^d dz \sin\left(\frac{\pi n z}{d}\right)\sin\left(\frac{\pi n' z}{d}\right) \\ &\times \int_0^d dz' \sin\left(\frac{\pi m z'}{d}\right)\sin\left(\frac{\pi m' z}{d}\right)\exp(-q|z-z'|). \end{aligned} \tag{3.10}$$

A dependence of the q^{-1} type leads to a divergence of each graph for low values of q, although—as can be seen from Eq. (3.9)—the quantity $S^{(2)}$ itself is finite in this limit. The finite nature of $S^{(2)}$ is ensured by inclusion of graphs of the *abcc* type, in which holes also generate phonons. We shall consider only the case when an electron generating phonons remains in the same size-quantization band. The terms which are not diagonal in respect of the band indices make a smaller contribution, as shown in Ref. 19. It follows from Eq. (3.10) that[13]

$$I_{nn}^{nn}(q)\equiv I_n(q)=2\pi\alpha_0 l_0 \omega_{LO}^2 S_0^{-1} F_n(q), \tag{3.11}$$

$$F_n(q)=\frac{8}{q}[(qd)^2+(2\pi n)^2]^{-1}\left[\frac{3}{8}qd+\frac{(\pi n)^2}{qd}-\frac{4(\pi n)^4}{(qd)^2}\frac{1-\exp(-qd)}{(qd)^2+(2\pi n)^2}\right],\quad n=1,2\ldots \tag{3.12}$$

If $q\to 0$, then $F(q)\to q^{-1}$; if $q\to\infty$, we obtain $F(q)\propto q^{-2}$, which ensures convergence of the integrals at high values of q. In the model interaction case,[6] we have

$$I(q)=12\pi Ad^2\omega_{LO}{}^2S_0^{-1}\equiv I. \tag{3.13}$$

Since I is independent of q, the graphs converge at low values of q.

In the adopted approximation, we find that I is independent of the discrete quantum number n. According to Eqs. (3.11) and (3.12), the scattering tensor of Eq. (3.9) becomes

$$S^{(2)}=2B(2\pi\alpha_0 l_0\omega_{LO}{}^2)^2\delta(\omega_l-\omega_s-2\omega_{LO})S_0^{-1}\times\sum_n\sum_q F_n(q)\,|A_1(n,q)-A_2(n,0)|^2,$$

$$A_1(n,q)=A_1(n_\mu=n,\ n_\nu=n,\ q),\quad A_2(n,0)=A_1(n,0). \tag{3.14}$$

In the approximation of the model interaction the graphs a_1a_1 and a_2a_2 make the contribution [see Eq. (3.1)]:

$$S^{(2)}_{a_1a_1}+S^{(2)}_{a_2a_2}=2B(12\pi Ad^2\omega_{LO}{}^2)^2\delta(\omega_l-\omega_s-2\omega_{LO})S_0^{-1}\times\sum_{nq}|A_1(n,\mathbf{q})|^2. \tag{3.15}$$

Integrating with respect to the two-dimensional vector $\mathbf{k}$ in Eq. (3.8), we obtain the exact expression for the function $A_1(n,q)$:

$$A_1(n,q)=A_{11}(n,q)-A_{12}(n,q), \tag{3.16}$$

$$A_{11}(n,q)=\frac{a_0}{z_1^{1/2}}\ln\left[\frac{p_2^2(z_1^{1/2}+p_2^2-p_1^2-q^2)}{z_1^{1/2}(p_1^2-q^2)-(p_1^2-q^2)^2+p_2^2(p_1^2+q^2)}\right]; \tag{3.17}$$

A_{12} is found from A_{11} by the substitutions $z_1\to z_2$ and $p_2\to p_0$;

$$z_1=q^4-2(p_2^2+p_1^2)q^2+(p_2^2-p_1^2)^2,$$

$$z_2=q^4-2(p_0^2+p_1^2)q^2+(p_0^2-p_1^2)^2, \tag{3.18}$$

$$a_0=(2\pi\omega_{LO})^{-1}(2m_e/\hbar^2)^2,\quad p_j^2=\frac{2m_e}{\hbar}(\omega_j-n^2\omega_e+i\gamma_n/2),$$

$$j=0,1,2.$$

We shall represent A_{11} and A_{12} in the form

$$A_{11}(n,q)=\frac{a_0}{z_1^{1/2}}(\ln p_2^2+f_1),\quad A_{12}(n,q)=\frac{a_0}{z_2^{1/2}}(\ln p_0^2+f_2), \tag{3.19}$$

where f_1 and f_2 are smooth logarithmic functions. It is clear from Eqs. (3.18) and (3.19) that if the frequency ω_l satisfies the condition

$$\omega_l=\omega_g+n^2\omega_e+2\omega_{LO},\quad \omega_e=\pi^2\hbar/2m_ed^2, \tag{3.20}$$

then Re $p_2^2\to 0$ and a factor $\ln A^2$ appears in Eq. (3.15), i.e.,

$$S^{(2)}_{aa}+S^{(2)}_{a'a'}=2B(16\pi^2d^2\omega_{LO}{}^2a_0A\ln A)^2\delta\times(\omega_l-\omega_s-2\omega_{LO})S_0^{-1}\sum_{nq}z_1^{-1}. \tag{3.21}$$

If the resonance condition of Eq. (3.20) is not obeyed, then $\ln p_2^2$ is not a large quantity and we have

$$S^{(2)}_{a_1a_1}+S^{(2)}_{a_2a_2}\propto A^2. \tag{3.22}$$

Therefore, logarithmic enhancement of the intensity of the second phonon replica occurs at a resonance. This enhancement is due to the fact that a range of the momenta in the vicinity of a minimum of the two-dimensional band, where the density of states diverges logarithmically, participates in electron transitions.

Graphs *ab*, *ba*, and *bb* considered in the heavy hole approximation diverge for the model interaction in the range of large phonon momenta. Their convergence is achieved by including the hole energy in G_h and $\tilde{G}_h$. It is sufficient to retain the term $\hbar^2q^2/2m_h$, because then the graphs in question depend on the coupling constant A in the same way as in Eq. (3.21).

In the case of the Fröhlich interaction, $S^{(2)}$ includes, according to Eq. (3.17), the functions

$$A_{11}(n,0)=\frac{a_0}{p_2^2-p_1^2}\ln\frac{p_2^2}{p_1^2},\quad A_{12}(n,0)=\frac{a_0}{p_0^2-p_1^2}\ln\frac{p_0^2}{p_1^2}. \tag{3.23}$$

Using Eq. (3.19), we can rewrite $S^{(2)}$ in the form

$$S^{(2)}=2B(2\pi\omega_{LO}{}^2a_0\alpha_0)^2\delta(\omega_l-\omega_s-2\omega_{LO})S_0^{-1}\sum_n\sum_q F_n{}^2(q)\times\left|\left(\frac{1}{z_1^{1/2}}+\frac{\hbar}{2m_e\omega_{LO}}\right)\ln\frac{p_2^2}{p_1^2}-\left(\frac{1}{z_2^{1/2}}-\frac{\hbar}{2m_e\omega_{LO}}\right)\ln\frac{p_0^2}{p_1^2}\right|^2. \tag{3.24}$$

If the resonance condition of Eq. (3.20) is satisfied, then $S^{(2)}\propto(\alpha_0\ln\alpha_0)^2$. Therefore, both types of interaction give rise to the same dependence on the coupling constant.

We shall conclude this section by noting that our results are based on the assumption that throughout the size-quantization band the broadening of the electron states is governed by the constant $\gamma_n\sim\alpha_0$, i.e., it is governed by the spontaneous emission of an LO phonon. However, in the first band in the vicinity of its minimum the emission of LO phonons is forbidden and the broadening is governed by other scattering mechanisms (for example, the scattering by impurities). In contrast to the three-dimensional case,[7] this results in enhancement of the contribution made to the phonon replica peak by the first band, since the constant $\gamma'<\gamma_n$ occurs in the logarithm.

4. HIGHER-ORDER PHONON REPLICAS

We shall consider briefly the graphs corresponding to phonon replicas with $N\geqslant 3$, which are accompanied by the emission of three or more phonons. The total number of

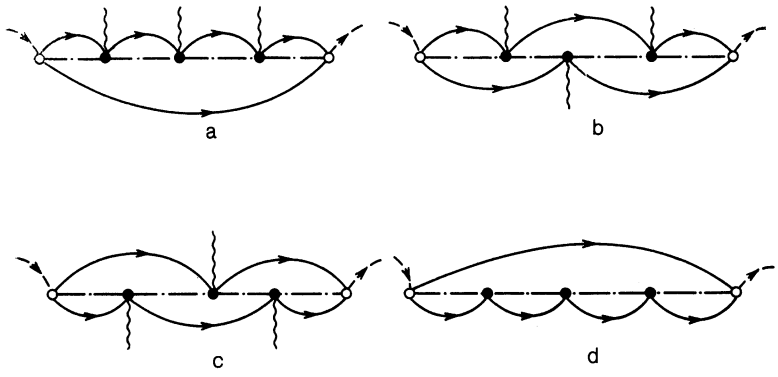

FIG. 3. Elements of graphs for the third phonon replica; Figs. 3a–3d correspond to the elements *a–d*.

graphs describing phonon replicas with the number N is $(N+1)^2N!$, where $(N+1)^2$ is equal to the number of different types of graphs and $N!$ is the number of different combinations of the outer phonon lines of a given type (ranging from "ladder" to "fan"). The four elements of which the graphs are composed in the $N=3$ case are shown in Fig. 3. There is a total of 16 types of graphs. Out of these there are eight types with an odd number of the whole lines and they are negative, so that mutual canceling of the graphs takes place. None of the graphs show divergence at low momenta in the case of the Fröhlich interaction. We shall consider in greater detail two graphs of the *aa* type: a "ladder" graph a_1a_1 and a "fan" graph (Fig. 4). They correspond (the sum with respect to n is not included)

$$S_{a_1a_1}^{(3)}=B\delta(\omega_l-\omega_s-3\omega_{LO})\sum_{\mathbf{q}_1\mathbf{q}_2}I(q_1)I(|\mathbf{q}_1-\mathbf{q}_2|)|A_3(q_1,\mathbf{q}_2)|^2, \tag{4.1}$$

$$S_{a_2a_2}^{(3)}=B\delta(\omega_l-\omega_s-3\omega_{LO})\times\sum_{\mathbf{q}_1\mathbf{q}_2}I(q_1)I(|\mathbf{q}_1-\mathbf{q}_2|)I(\mathbf{q}_2)A_3(q_1,\mathbf{q}_2)A_3^*(q_3\mathbf{q}_1), \tag{4.2}$$

$$A_3(q,\mathbf{q}')=\sum_{\mathbf{k}}G_e(n,\mathbf{k},\omega_0)G_e(n,\mathbf{k}-\mathbf{q}_1,\omega_1)G_e\times(n,\mathbf{k}+\mathbf{q}_2,\omega_2)G_e(n,\mathbf{k},\omega_3). \tag{4.3}$$

We shall now analyze the model interaction when $I(q)$ is independent of the phonon momentum $[I(q)\propto A]$. After substitution of the variables

$$\mathbf{k}_\mu=\mathbf{k}_0,\ \mathbf{k}_\mu-\mathbf{q}_1=\mathbf{k}_1,\ \mathbf{k}_\mu+\mathbf{q}_3=\mathbf{k}_2,\ \mathbf{k}_n=\mathbf{k}_0+\mathbf{p}, \tag{4.4}$$

Eq. (4.1) becomes

$$S_{a_1a_1}^{(3)}=B\delta(\omega_l-\omega_s-3\omega_{LO})I^3S_0^{-1}\times\sum_{\mathbf{p}}Y_n(\omega_1,\omega_1,\mathbf{p})Y_n(\omega_2,\omega_2,\mathbf{p})Z(n,\mathbf{p}), \tag{4.5}$$

$$Y_n(\omega_i,\omega_j,\mathbf{p})=\sum_{\mathbf{k}}G_e(n,\mathbf{k},\omega_i)G_e(n,\mathbf{k}_j+\mathbf{p},\omega_j),\quad j=1,2, \tag{4.6}$$

$$Z(n,\mathbf{p})=\sum_{\mathbf{k}_0}G_e(n,\mathbf{k}_0,\omega_0)\bar{G}_e(n,\mathbf{k}_0+\mathbf{p},\omega_0)G_e(n,\mathbf{k}_0,\omega_3)\bar{G}_e\times(n,\mathbf{k}_0+\mathbf{p},\omega_3). \tag{4.7}$$

The fan graph of Eq. (4.2) contains not the functions $Y_n(\omega_i,\ \omega_i,\ p)$, but

$$Y_n(\omega_1,\ \omega_2,\ p)Y_n(\omega_2,\ \omega_1,\ p). \tag{4.8}$$

The substitution of the variables described by Eq. (4.4) reduces the problem to calculation of the integrals already encountered in Sec. 3. Expanding the function $Z(n,p)$ into the simplest fractions, we can describe it in the form of a sum of the functions (4.6):

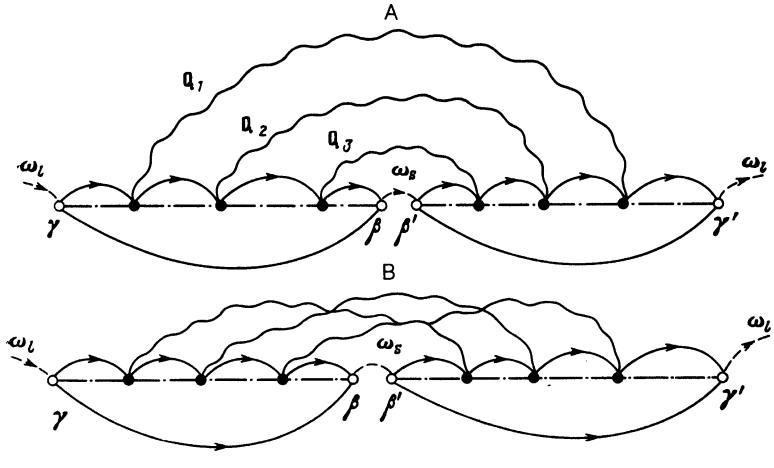

FIG. 4. Graphs for the third phonon replica: *A* is the graph a_1a_1 (of the ladder type) and *B* is the graph a_2a_2 (of the fan type).

$$Z(n,p)=(\omega_0-\omega_3)^{-2}\{Y_n(\omega_3,\omega_3,p)+Y_n(\omega_0,\omega_0,p)-Y_n(\omega_3,\omega_0,p)-Y_n(\omega_0,\omega_3,p)\}. \quad (4.9)$$

Integration of Eq. (4.6) gives

$$Y_n(\omega_i,\omega_j,p)=\frac{a_0}{z_{ij}^{1/2}}\ln\left\{\frac{p_j^2(z_{ij}^{1/2}+p_j^2-p_i^{*2}-p^2)}{z_{ij}^{1/2}(p_i^{*2}-p^2)-(p_i^{*2}-p^2)^2+p_j(p_i^{*2}+p^2)}\right\} \quad (4.10)$$

$$z_{ij}=p^4-2(p_j^2+p_i^{*2})p^2+(p_j^2-p_i^{*2})^2 \quad (4.11)$$

(p is the integration variable).

Equation (4.5) contains terms with a product of three functions Y_n characterized by identical ω_i. These terms correspond to the channels of direct creation and direct annihilation of an EHP. Since the polynomials z_{ij} in the functions $Y_n(\omega_i,\omega_i,p)$ are transformed into

$$z_{ii}=p^4-4\,\mathrm{Re}\,p_i^2p-(\gamma_n^2/4)(2m_e/\hbar)^2, \quad (4.12)$$

it follows that the sum (4.5) is dominated by the terms $p\propto\gamma_n^{1/2}$ and that a factor $\gamma_n^{-1}\propto A^{-1}$ (A is the coupling constant) appears in this sum, i.e., $S^{(3)}_{a_1a_1}\propto A^2$. In the case of the other two terms the range of large values is $p\gg\gamma_n^{1/2}$ and their contribution are described by $S^{(3)}_{a_1a_1}\propto A^3$. In the fan graph, as can be seen from Eq. (4.8), there is only one function Y_{ii} with coincident frequencies and, therefore, $S^{(3)}_{a_2a_2}\propto A^3$. It therefore follows that in the case of a phonon replica with $N=3$ the largest contribution is made by the ladder-type graphs.

Generalization to higher-order phonon replicas is self-evident. An increase in the order of a phonon replica by unity gives rise to an additional function $Y(\omega_i,\omega_i,p)$ in the integral and this makes an additional contribution of γ_n^{-1}. Consequently, the extra degree of the coupling constant in the numerator is compensated by a factor $\gamma_n\propto A$ in the denominator. Therefore, all the phonon replicas beginning from $N=2$ are, with an accuracy to within logarithmic multipliers, proportional to the square of the coupling constant. The greatest contribution comes from a ladder-type graph and it corresponds to

$$S^{(N)}_{a_1a_1}=B(12\pi d^2\omega_{LO}^2a_0A)^N\delta(\omega_l-\omega_s-N\omega_{LO})S_0^{-1}\times\sum_n\sum_p\prod_{j=1}^{N-1}Y_n(\omega_j,\omega_j,p)Z(n,p). \quad (4.13)$$

This expression is equal to that given in Ref. 12, but with different notation. Since for $N-2$ the functions $Y(\omega_j,\omega_j,p)$ make a contribution proportional to $\gamma_n^{-(N-2)}$, we have $S^{(N)}_{a_1a_1}\propto A^2$. If the frequency ω_i approaches $\omega_g+n^2\omega_e+N\omega_{LO}$, then the function $Y_n(\omega_N,\omega_N,p)$ in $Z(n,p)$ gives rise to a factor $\ln A$. Therefore, as in the $N=2$ case, the intensity of the phonon replica peak should rise logarithmically. Graphs of the *ad* and *dd* type (Fig. 3) make small contributions, since they do not allow for resonances (the appearance of N functions Y_n with identical frequencies). Therefore, these contributions are proportional to a higher degree of the coupling constant.

In this section we considered only the model interaction. The Fröhlich interaction does not alter qualitatively the conclusions reached above, since a phonon replica with $N\geqslant3$ does not give rise to divergence of the graphs at low photon momenta. Therefore, there is no need to include all the graphs, as had been done in Sec. 3 in the case of the second phonon replica.

5. DISCUSSION OF RESULTS

We shall now consider briefly the main results of our investigation. The fact that the phonon replicas depend on the coupling constant with the same power exponent, which is true beginning from a certain number, had been proved earlier for the scattering in a bulk semiconductor in the absence and presence of a strong magnetic field. The main result of the above theory is identification of the specific behavior of phonon replicas in a quasi-two-dimensional quantum well. This is due to, firstly, a reduction in the dimensionality of the region where an electron "wanders" generating phonons (plane instead of volume) and, secondly, due to a logarithmic singularity of the density of states in a two-dimensional size-quantization band. The first circumstance has the effect that an increase in the degree of the coupling constant ceases beginning from the third phonon replica, which is proportional to the α_0^2 (in the bulk case this begins from the fourth phonon replica, which is proportional to α_0^3). Therefore, the theory predicts a strong increase in the specific (per unit volume of the scattering region) intensity of phonon replicas in the case of the Raman light scattering in a quantum well, compared with the scattering in a bulk sample. In the case of GaAs, which is characterized by $\alpha_0\approx2\times10^{-2}$, such an increase in the intensity can be by a factor of many tens of times. Since the first phonon replica is weak (it is absent in the dipole approximation), it follows that the intensities of all the phonon replicas ($N\geqslant2$) should depend with the logarithmic precision in the same way on the electron–phonon coupling constant. This should make it possible to detect experimentally the distant phonon replicas.

A logarithmic singularity of the density of states gives rise to a factor $\ln^2\alpha_0$ (for $N=2$) and $\ln\alpha_0$ (for $N\geqslant3$) in the expression for the intensity of a phonon replica, if the frequency of the exciting light ω_l approaches $\omega_g+n^2\omega_e+N\omega_{LO}$. The frequencies ω_l and ω_s are in this theory related closely to the condition $\omega_l=\omega_s+N\omega_{LO}$, i.e., the phonon replica peaks are infinitesimally narrow. This is a consequence of our neglect of the phonon dispersion.

[1] M. Cardona and G. Güntherodt (eds.), *Light Scattering in Solids*, IV, Springer-Verlag, Berlin (1984).
[2] P. Manuel, G. A. Sai-Halasz, L. L. Chang *et al.*, Phys. Rev. Lett. **37**, 1701 (1976).
[3] R. Merlin, G. Güntherodt, and R. G. Humphreys, Proc. Fourteenth Intern. Conf. on Physics of Semiconductors, Edinburgh, 1978, publ. by Institute of Physics, London (1979), p. 875 [Institute of Physics Conf. Series, Vol. 43].
[4] M. Yoshida, N. Ohno, M. Mitsutake *et al.*, J. Phys. Soc. Jpn. **24**, 2754 (1985); N. Ohno, M. Yoshida, K. Nakamura, and Y. Nakai, Solid State Commun. **53**, 569 (1985).
[5] R. M. Martin, Phys. Rev. B **10**, 2620 (1974).
[6] R. Zeyher, Solid State Commun. **16**, 49 (1975).
[7] A. V. Goltsev, I. G. Lang, S. T. Pavlov, and M. F. Bryzhina, J. Phys. C **16**, 4221 (1983).
[8] I. G. Lang, S. T. Pavlov, A. V. Gol'tsev, and M. Ramos, Fiz. Tverd. Tela (Leningrad) **24**(6), 1744 (1982) [Sov. Phys. Solid State **24**, 993 (1982)].

[9] V. I. Belitskiĭ, A. V. Gol'tsev, I. G. Lang, and S. T. Pavlov, Zh. Eksp. Teor. Fiz. **86**, 272 (1984) [Sov. Phys. JETP **59**, 155 (1984)].
[10] T. Ruf and M. Cardona, Phys. Rev. Lett. **63**, 2288 (1989).
[11] R. P. Seĭsyan and Sh. U. Yuldashev, Fiz. Tverd. Tela (Leningrad) **30**, 12 (1988) [Sov. Phys. Solid State **30**, 6 (1988)].
[12] L. I. Korovin, S. T. Pavlov, and B. É. Éshpulatov, Pis'ma Zh. Eksp Teor. Fiz. **51**, 516 (1990) [JETP Lett. **51**, 584 (1990)].
[13] L. I. Korovin, S. T. Pavlov, and B. É. Éshpulatov, Fiz. Tverd. Tela (Leningrad) **30**, 3665 (1988) [Sov. Phys. Solid State **30**, 2105 (1988)]; Preprint No. 1400 [in Russian], Physicotechnical Institute, Academy of Sciences of the USSR, Leningrad (1989), p. 50.
[14] K. Trallero Giner, I. G. Lang, and S. T. Pavlov, Fiz. Tverd. Tela (Leningrad) **23**, 1265 (1981) [Sov. Phys. Solid State **23**, 743 (1981)].
[15] R. Enderlein, K. Peuker, and F. Bechstedt, Phys. Status Solidi B **92**, 149 (1979).
[16] J. E. Zucker, A. Pinczuk, D. S. Chemla *et al.*, Phys. Rev. Lett. **51**, 1293 (1983).
[17] E. L. Ivchenko, I. G. Lang, and S. T. Pavlov, Fiz. Tverd. Tela (Leningrad) **19**, 2751 (1977) [Sov. Phys. Solid State **19**, 1022 (1977)].
[18] A. V. Gol'tsev, I. G. Lang, and S. T. Pavlov, Fiz. Tverd. Tela (Leningrad) **22**, 2766 (1980) [Sov. Phys. Solid State **22**, 1612 (1980)].
[19] S. Das Sarma and B. A. Mason, Ann. Phys. (NY) **163**, 78 (1985).
[20] B. K. Ridley, J. Phys. C **15**, 5899 (1982).

Translated by A. Tybulewicz